



HOCHSCHULE LANDSHUT
HOCHSCHULE FÜR ANGEWANDTE WISSENSCHAFTEN



AN-INSTITUT FÜR ANGEWANDTE NUTZFAHRZEUGFORSCHUNG UND ABGASANALYTIK (*BELICON*)
GESCHÄFTSFÜHRER: PROF. DR.-ING. RALPH PÜTZ

Operational Analysis with a HIGER-Electrobus with AOWEI-Supercaps using Energy Consumption Data in Real Operation on an Urban Bus Route in Sofia together with accompanying simu- lation calculations

Produced on behalf of


Chariot Motors AD

Sofia 1000, Stolichna Municipality, Sredets Region,

10 Tsar Osvoboditel Blvd., 3rd floor

Report No. BELICON/CHMO-1-25.10.2014

This report may only be published in its entirety without omissions and additions. If sections are reproduced or photocopied, then the written permission of the author must be sought.

Published by	Prof. Dr.-Ing. R. Pütz	25.10.2014	<i>R. Pütz</i>
Produced by	Prof. Dr.-Ing. A. Kleimaier Prof. Dr.-Ing. R. Pütz Th. Haberstock, B.Eng. P. Lorenz		

Contents

- 1 Scope of Work 4**
- 2 Test Vehicle Applied 5**
- 3 Selected Route 7**
- 4 Energy Consumption Measurements on Line 11 in
real operation..... 10**
 - 4.1 Implementation of the Measurements 10
 - 4.2 Implementation of the Analysis 14
 - 4.3 Analysis of the Assessment Results 15
 - 4.3.1 Operational Profile and Speed..... 15
 - 4.3.1.1 Performance in Intermediate Circuit 18
 - 4.3.2 Energy Consumption 24
 - 4.4 Summary..... 29
- 5 Simulated Calculation of the Energy Demand on Line 11 29**
 - 5.1 Description of the Simulation Model Applied..... 29
 - 5.2 Simulation of the Energy Demand on Line 11 32
 - 5.2.1 Scenario 1: 100% Occupancy Rate 32
 - 5.2.2 Scenario 2: 25% Occupancy Rate 34
 - 5.3 Summary Tables showing the most important simulation energy demand
results 35

1 Scope of Work

Normally electric mobility presents an individual system for each transport operator and its operational parameters, whereby the vehicle technology, propulsion system, type and energy content of the energy storage unit, energy input type/filling process and operational design must be harmonised with the respective route topology. Thus, the different approaches ranging from an established trolley bus with a permanent overhead wiring fixture to the various contact-free systems are manifold. With the contact-free systems a differentiation is made in the glossary between the options 'Opportunity Electrobus' and 'Overnight Electrobus'.

An Overnight Electrobus has a large energy storage unit so that the entire daily route stretch of an urban bus – as is the case with a conventional diesel bus – can be completed during the day without any additional energy input. Usually in this case, a battery is used as the energy storage unit due to the large volume of energy required, and this can be charged slowly and gently overnight. However, the operational advantage of this option is outweighed by the fact that the weight of the energy storage unit significantly reduces the passenger capacity which would mean additional vehicles having to be used on the busiest routes in the city.

On the other hand, an Opportunity Electrobus only has a small energy storage unit which means passenger capacity can be maximised. However, this option requires frequent recharging during vehicle operation. This in itself presents heavy demands on the performance density of the energy storage unit due to the extremely limited time for charging during route operation as it has to absorb a large quantity of energy within a very short period which reduces the lifespan of the battery. Significant ease of use would be offered by an energy storage unit which combines a typical battery high energy density with the high power density of an Ultra-Capacitor (Supercaps).

The company Chariot Motors, who commissioned this report, offers this type of energy storage system based on its own data, with similarly high power and energy densities. This involves an innovative Ultra-Capacitor with an energy content of 20 kWh which only weighs around 900 kg. The manufacturer of the Supercap is the company

AOWEI in Shanghai. With this type of system a sufficiently high passenger capacity would be feasible for an Electrobus with little impact on route operation due to the short charging times. Within the framework of this study, the performance the efficiency of the new Supercap - fitted to an Electrobus made by the manufacturer HIGER - will be tested on the urban bus line 11 in Sofia during routine bus operation. For this purpose, energy consumption measurements will be carried out en route. Additional simulation calculations should enable consideration of limit levels. The entire vehicle will, hereafter, be referred to as 'Chariot eBus'.

2 Test Vehicle Applied



Figure 2-1: Chariot eBus during test runt

The vehicle to be tested is a Solobus manufactured by the Chinese company HIGER Bus Company Limited and it has an electrical central power drive for traction power. The bus is a 12m long Solobus with two doors and signage with 'Chariot eBus'. This is purely electric and can be charged optionally via a plug-in charger or, preferably, through a pantograph from the overhead wiring. A modern ultra-capacitor (Ultra-Cap) manufactured by AOWEI supplies two Siemens electric motors, which are linked to the conventional low floor gantry axles via a summation gear. The respective technical data is presented in the following table.

Technical Data	
Manufacturer	HIGER Bus Company Limited
Type	Chariot eBus
Seats / Standing Places	27 / 53
Length / Width / Height [mm]	1200 / 2550 / 3680
Wheelbase [mm]	5500
Unladen weight [kg]	12540
Technically permissible overall weight [kg]	18000
Engine / Torque [Nm]	2x E-Engine (Siemens) / 2x 430
Energy storage units	Ultra-Cap (AOWEI, China)
- Capacity [kWh]	20
- Weight [kg]	<< 1000
Air conditioning	Thermo King E-Aircon (26kW)
Heating	Spheros E320 (32kW)

Table 2-1: Technical data: Chariot eBus (Source: Spec Sheet Chariot eBus)

For the purpose of electrically charging the bus, two charging stations have been erected on Line 11 in Sofia. The first charging station is situated at the start of the route at the vehicle depot; the second is at the turning point where Line 11 starts its reverse journey. The charging units are supplied through the existing trolleybus overhead wiring with a direct current voltage of up to 680 V. In this process, heavy fluctuations in the current are common. The bus is charged at each of the charging stations via a pantograph. Figure 2.2 shows the docking of the pantographs at the charging stations.



Figure 2-2 Pantograph Docking at the Charging Stations

Once the Pantograph has been connected the charging station automatically administers the charging process. Once the required capacity has been reached, the bus suspends the charging process by reversing the pantograph. Since the balance of the individual capacitor modules fluctuates during the charging process, charging is generally halted even before 100% capacity has been reached, i.e. as soon as one of the capacitors has reached maximum load.

Due to these circumstances the degree of efficiency of the charging stations cannot be determined and is not taken into account in the following consideration. Likewise, the diesel consumption of the on-board heating (manufactured by Spheros) is unknown and cannot therefore be entered into the balance.

3 Selected Route

Since the Chariot eBus is to be tested during routing bus operation in Sofia, the energy consumption recording on this line should be representative, i.e. take place with passengers present. As there are two charging stations, this involves bus Line 11 which consists of one full circuit from two cycles respectively - one cycle from the depot to the end of the route and another cycle following charging, back to the charging station at the depot. Thus, one charging will suffice respectively for one circuit. The total route is approximately 22km long, which equates to a total route length of around 88km with 4 circuits per test day being travelled. The following diagram shows an example of the GPS data measurements taken on 08.10.2014 The Depot is marked as the starting point.

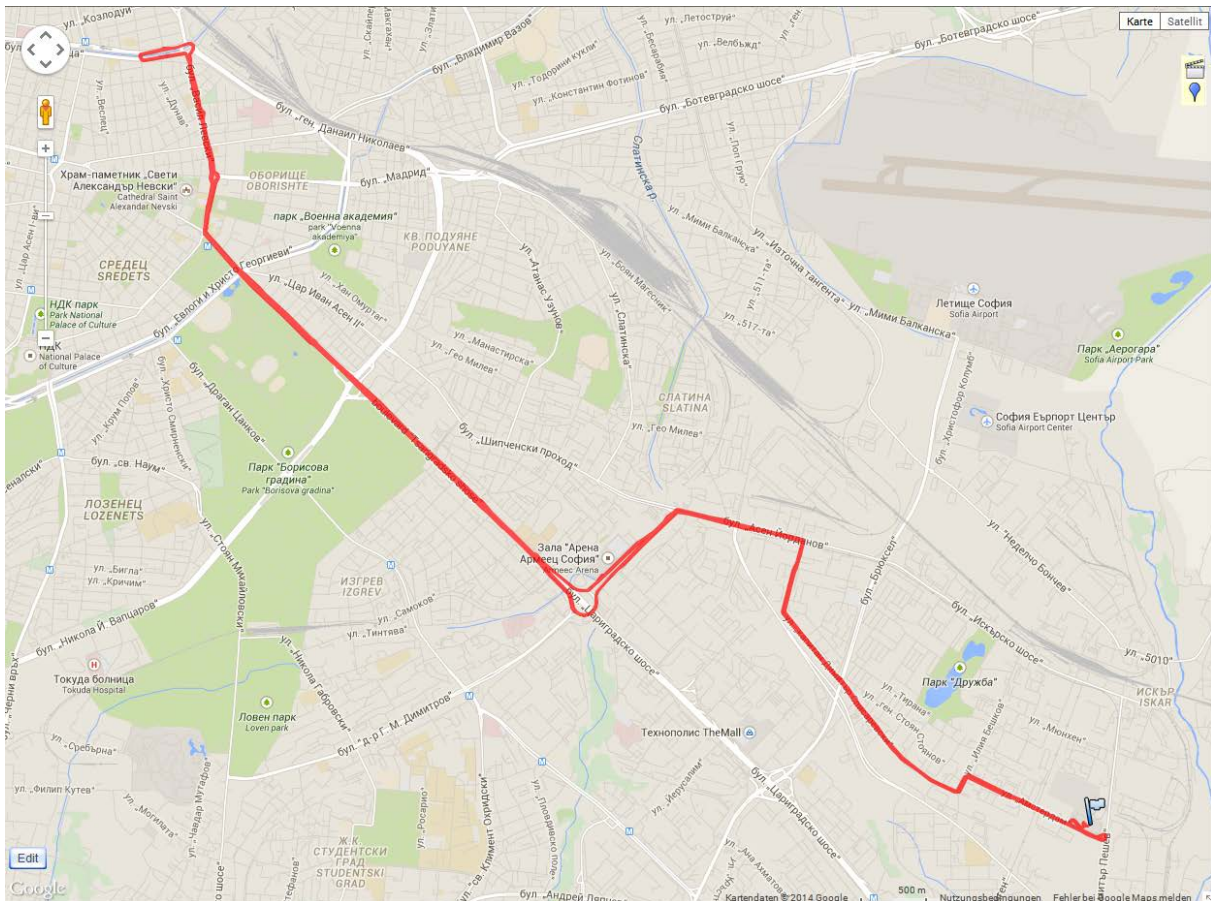


Figure 3-1: Test Line 11, Data from 08.10.2014 (Data: QTravel; Map: Google)

From this map it is clear, that by splitting the route into two cycles per circuit Line 11 can be contemplated in both directions of travel. Since, however, there is no significant deviation in route progression, the cycles can be balanced in total for the whole day.

The following Figure 3-2 shows an example of the gradient and speed profile of a cycle (e.g. Cycle 2, charging station at the turning point back to the charging station at the bus depot) The average cycle speed is 16km/h (not including standing times between cycles) and is thus in the range of SORT-2-Level. The route can be considered as more or less even.

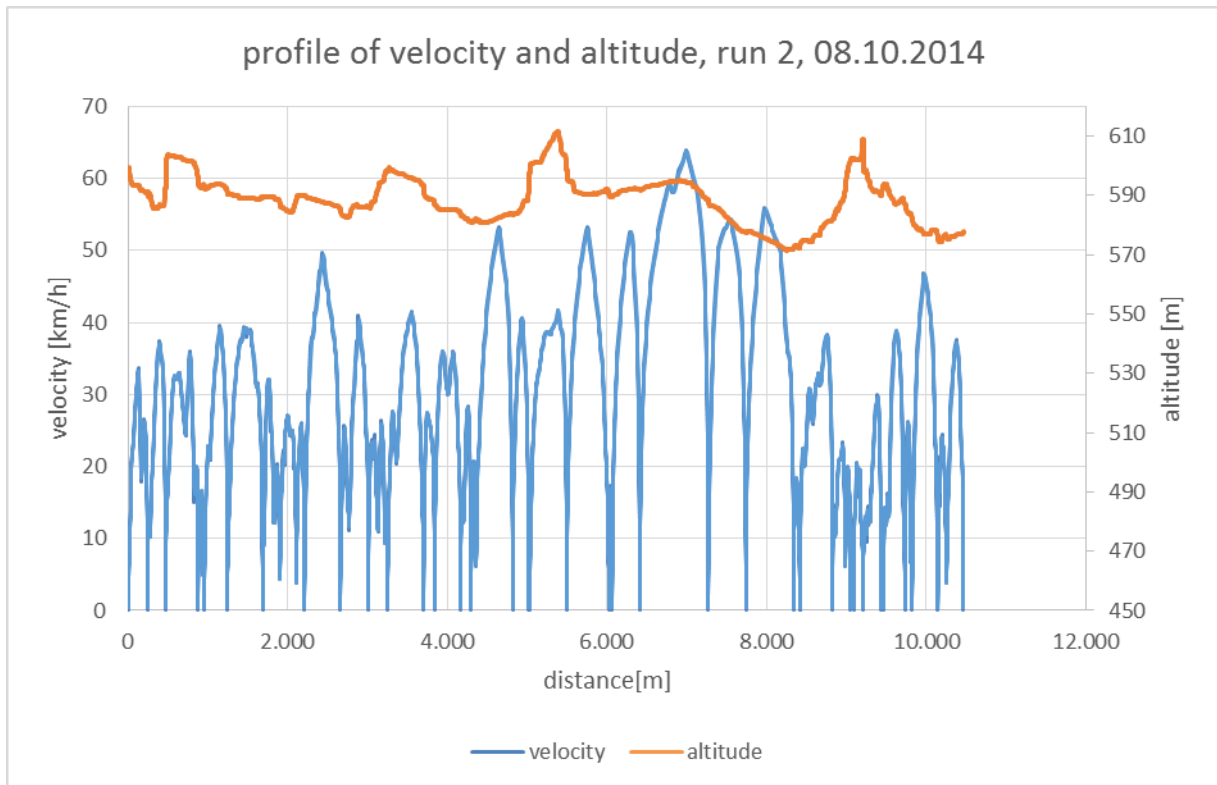


Figure 3-2: Speed-/Gradient Course of Line 11, Cycle 2, 08.10.14

In the following the temperature course from the 08.10.2014, as well as the area of measurement is presented. The temperatures during the test runs ranged from +12 to +14.5 °C, which had a negligible influence on the performance of the bus. Therefore, a differentiation on the basis of temperature influence is unnecessary.

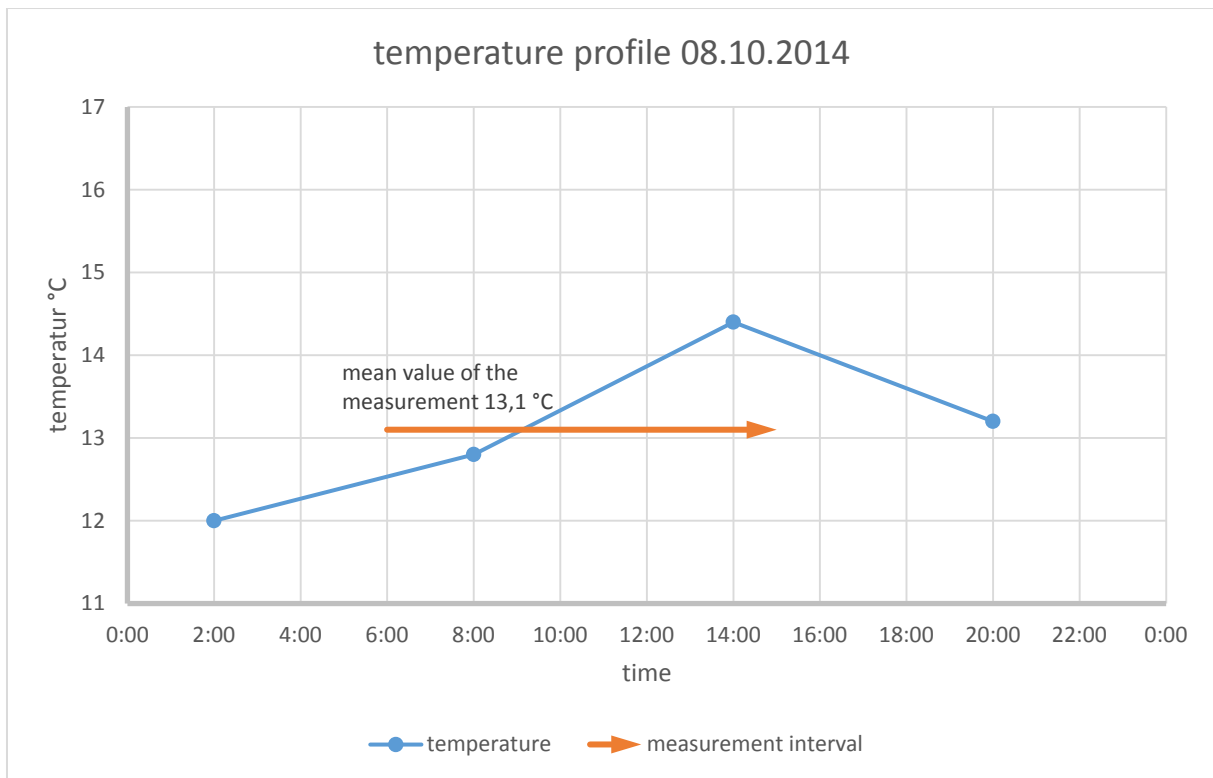


Table 3-1: Temperature Course, 08.10.14 (Data: Wetter.com)

4 Energy Consumption Measurements on Line 11 in real operation

4.1 Implementation of the Measurements

The measurements were taken during the period from 07.10.2014 to 08.10.2014. For 08.10 a complete set of data was recorded for the entire day's operation. The measurement from the 07.10 serves, in this respect, the purpose of calibrating the measuring equipment and validating the measurement results. Since the charging (energy input) takes place during the test run, the measurement recording within the vehicle means that a complete energy balance is available for one operational day.

In Figure 4-1 the on-board power supply of the test vehicle is presented in a simplified form. The high voltage on-board power supply (HV-network) works with a voltage of 400...600V DC and connects the Supercap directly to the pantograph or charging connection, thereby enabling the charging to take place. Both electric motors are supplied via the HV-network, which powers the rear axles via the summation gear. In

addition, the energy for the auxiliary consumers such as the air conditioning, air compressor, oil pumps, capacitor cooling etc. as well as the DCDC transformer for the 24 V low voltage on-board power supply is taken from the on-board power supply.

Three performance measuring devices with an internal data logger were used for the measurements:

- Chauvin Arnoux PEL 103
 - MP1 “Pantograph”
 - MP2 “Ultra-Cap”
 - MP3 “E-Motor”
- Chauvin Arnoux PEL 103
 - MP4 “Air conditioning unit”
 - MP5 “Air compressor + oil pump”
 - MP6 “24V on-board power supply”
- Fluke 345 Network analysis device
 - MP1: Cycles 1 to 4 / MP3: Cycles 5 to 8

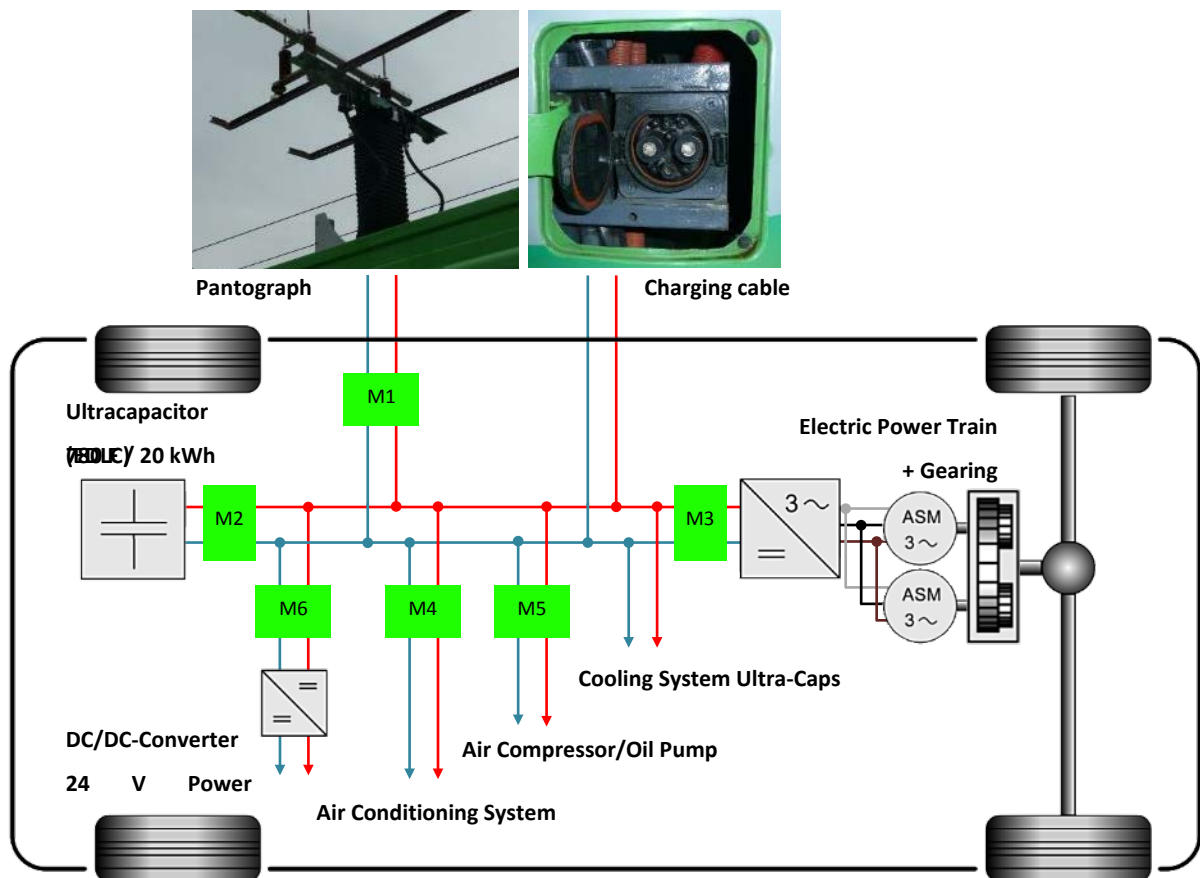


Figure 4-1: Measurement points within the vehicle

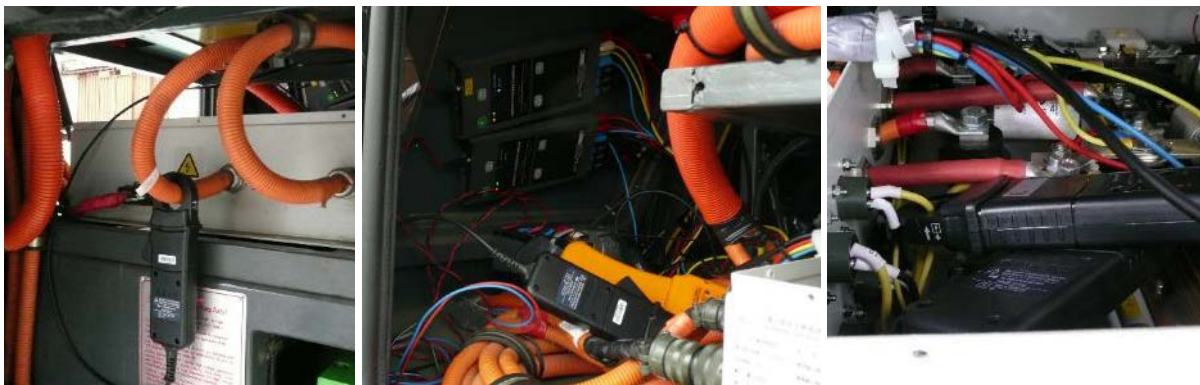


Figure 4-2: Operation of the Measuring Devices during Testing

For the measuring on the HV on-board power supply of the vehicle a suitable access was required. The distribution box for the electrics is easily accessible via a hatch at the rear and it can house all the test points. In Fig 4-2 above, the hatch is shown at the left rear side of the E-Bus. Below the hatch the integrated measuring instruments and cable attachments are shown.

The picture bottom left shows Measurement Point M2 which monitors the Supercaps. The middle picture shows both PEL 103 measuring devices fastened to the inside wall. The cable attachments in the bottom section measure the pantographs (M1) and the electric motor inverters (M3). Likewise, the FLUKE 345 (orange) can be seen, which is initially attached to the pantographs (M1) and, once half the cycles have been done, it is then attached to the feed pipe for the electric motors (M3).

The picture on the right shows the electricity cables in the converter box, which measure the DC/DC converter for the 24V on-board power supply and the supply to the air compressor and the oil pumps (M5). The connection to the air conditioning (M4) cannot be seen in the photos.

The cooling of the Supercaps is not measured. This is viewed as lost energy and can therefore not be presented in terms of the level of efficiency.

The three measuring devices make it possible to record the course of time for the electricity and voltage as well as the power and energy derived from it, including additional parameters. With adequate evaluation software the data gained can be fed into a PC, visualised and exported for further analysis in txt format. In addition, the time courses for the route and speed can be recorded using a GPS data logger (BT-Q1000XT) during the journeys. Since the measuring records can be synchronised through the time stamp recorded, a complete set of data for 08.10.2014 with the trajectory route, speed as well as performance and energy output is available for further evaluation.

For a better understanding at this point, the energy flow in the three system states: 'Charging', 'Driving' and 'Standstill' can be explained using Figure 4-1:

- During the charging process energy flows from the charging station via the pantograph (or network connection, not used during measurement) into the on-board power network. It then flows subsequently into the Supercap. In this case the energy flow from both measuring devices is recorded at M1 (pantograph) and M2 (Supercap). Due to losses as well as possible active additional consumers during loading, it is expected that the performance measured at M2 is lower.
- During travel the energy is exchanged bi-directionally between the Supercap and the drive; in such cases the device at M2 records the energy emitted by the Supercap as well as the energy absorbed by the electric motor inverters. Once again at this point, a lower performance at M3 due to losses and additional consumers can also be anticipated. In addition to classic engine operation the vehicle can also brake electrically and, thus, regeneratively. In this case, both E-machines work as generators: the kinetic energy from the vehicle – minus the conversion losses and additional consumer demand – flows back into the Supercap, thereby reducing the total consumption.
- Both in standstill operation as well as during travelling energy flows from the Supercap to the additional consumers. In standstill mode this can be directly analysed at M2. During travel, however, the measurements at M2 cannot differentiate between traction and additional consumer demand. Therefore additional measuring devices are incorporated at M4 (air conditioning unit), M5 (air compressor and oil pump) and M6 (DC/DC converter 24V on board network) so that the energy consumption of these additional consumers can be calculated precisely.

4.2 Implementation of the Analysis

The measurement data route/ speed was recorded in 1 second intervals (1 Hz), the measurement data for the performance / energy from the battery and network connection in 5 second intervals. NB: the measuring appliances are considerably more sensitive internally (Fluke 345: up to 15,625 kHz) and record average values for a more generalised time pattern in order to keep the data quantity within the processible limits. Fluke 345 can thus, for example, record in 5 s intervals for 26 hours. The data sets are read on the spot with the device software and exported in a general readable data format (.txt, .csv). The evaluation is done in conjunction with self programmed scripts (GNU Octave), which initially import the data and then process it further and analyse it as required. Following synchronisation with the time stamp the measurement values from all measuring appliances can be depicted over the same time basis.

Since the data sets for the journeys are very extensive and cover a huge time window, density functions for speed and performance are calculated for visualisation purposes. The analysis is divided into three sections with a concluding summary:

- **4.3.1 Vehicle Profile and Speed:**

Analysis of the speed trajectories of the individual journeys: these are necessary to evaluate the driving situation and serve as a basis for the calculation of the basic parameters of the specific energy consumption. The key data for duration, distance and speed are summarised in table format.

- **4.3.2 Performance in Intermediate Circuit:** Analysis of the power consumption / recuperation during the intermediate circuit for journeys (total journey) as well as for standstill periods (additional consumers). In order to check the plausibility the required wheel performance is estimated using a simplified longitudinal dynamics model.

- **4.3.3 Energy consumption:** Calculation of the energy turnover over an entire day and calculation of key consumption data as the concluding result of the analysis.

- **4.4 Summary:** brief presentation of the key data obtained.

4.3 Analysis of the Assessment Results

4.3.1 Operational Profile and Speed

On the 08.10.2014 4 line routes were driven and split into 8 cycles for analysis. Figure 4-3 plots the speed course of the first route journey across cycle 1 (outward) and cycle 2 (return). It can be seen that, during the journeys, depending on the traffic situation, a spatial displacement results between operational speed section profiles although these are parallel to the greatest possible extent.

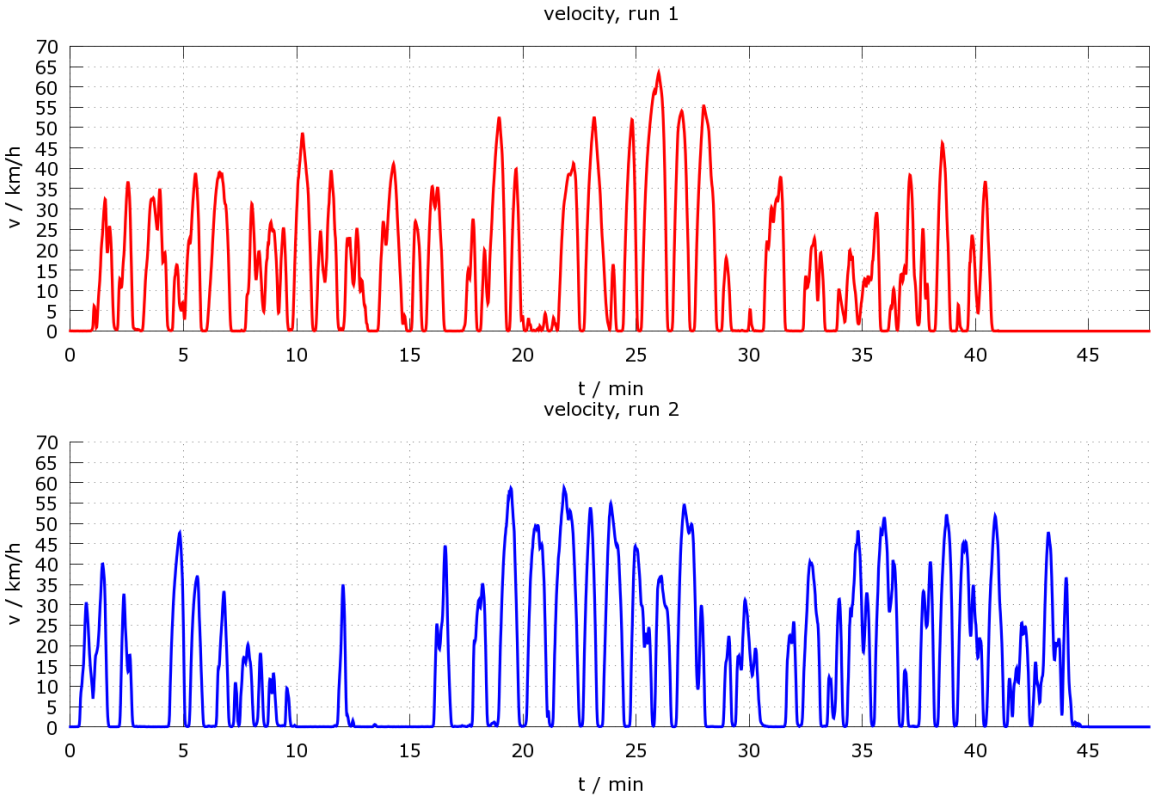


Figure 4-3: Total progression of Journeys 1 and 2 on the 08.10.2014

Figures 4-4 and 4-5 show a zoom in the first ten minutes of the journey, spread over time / route and should convey the effect of a typical pattern of the speed progression.

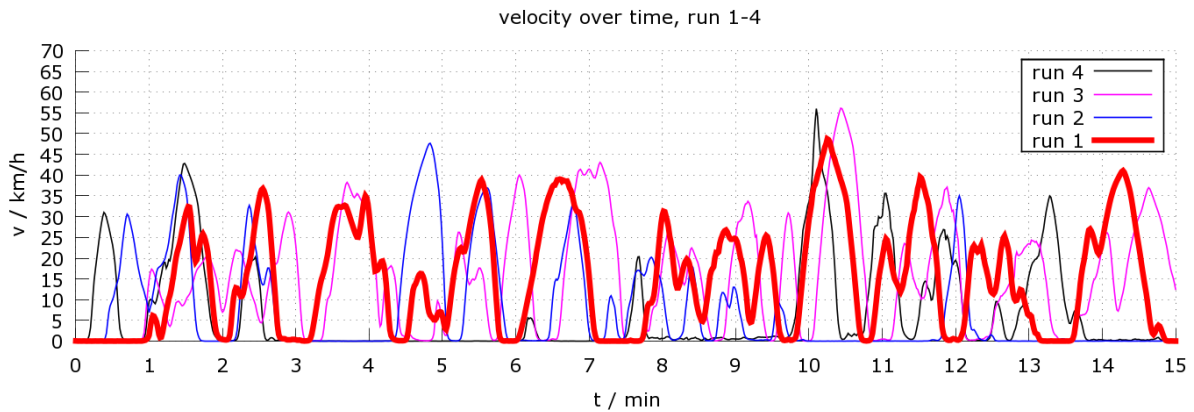


Figure 4-4: Progression of journeys 1 to 5 at the start of the cycle over time

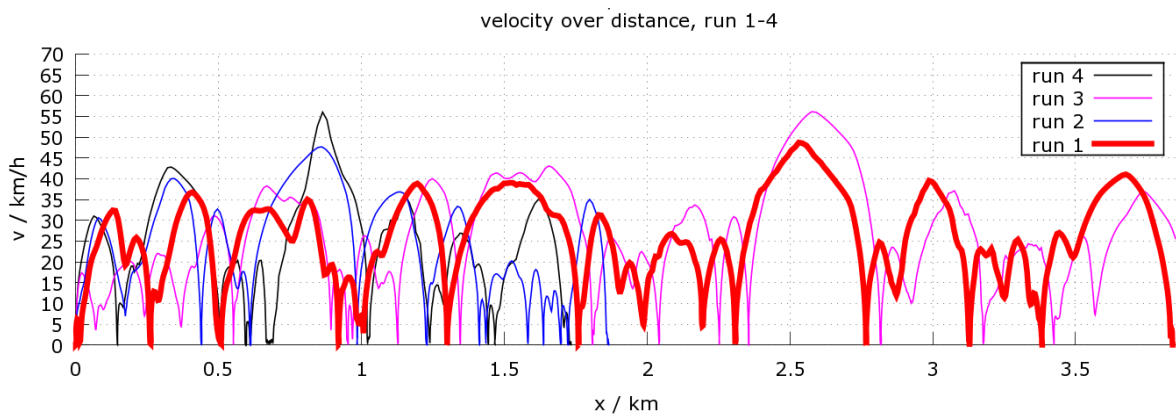


Figure 4-5: Progression of journeys 1 to 5 at the start of the cycle over distance

Since the individual time trend displays are unclear over and up to 48 min and, in addition, are difficult to compare with one another, the density functions for the speed spectrum of the individual journeys were calculated (see Figure 4-6). These correlate principally with the histograms usually applied with discrete bars; however, these are calculated continuously and therefore the resolution of the peaks in the process is noticeably finer. The programming and calculation effort is correspondingly higher.

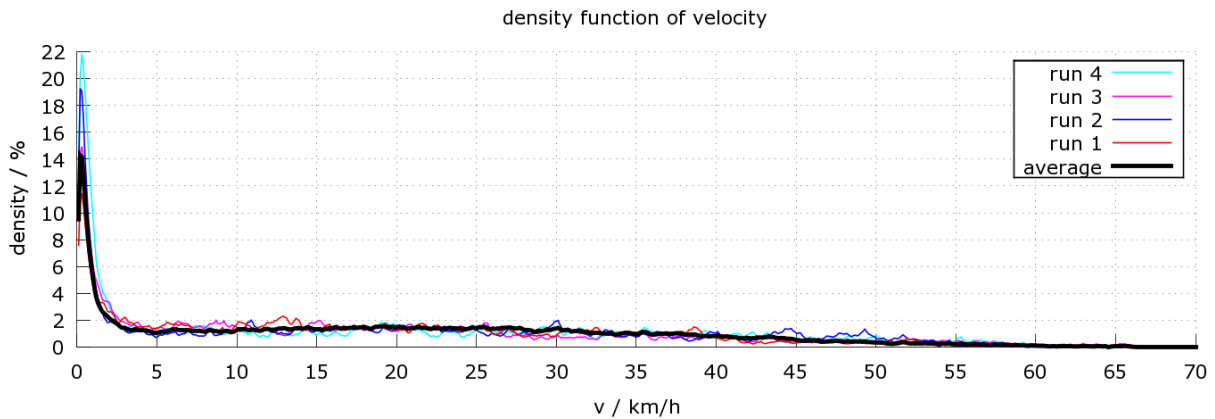


Figure 4-6: Spatial distribution of the velocity

Diagram 4-6 should be read as follows: the area beneath the curves corresponds to the portion of time when the vehicle is travelling at a particular speed interval. For the total range – in this case 0 to 70km/h – the area corresponds to 100% of the cycle period. The black curve here represents the average of all journeys. If the vehicle is travelling over a longer period in a fixed speed area, the density function presents this in the form of a peak. For Line 11, a peak of this type can only be seen for the standstill periods. Due to inaccuracies with small changes in position it is not set at exactly zero, instead there is a shift to the right. Otherwise the density function remains almost constant up to 30 km/h and only decreases slowly; at 60km/h hardly any time segments can be differentiated. Journeys at a constant speed would show up in the form of a peak and do not realistically occur – the journey profile consists almost solely of accelerating and braking whereby the corresponding speed area is driven through.

	Journey 1	Journey 2	Journey 3	Journey 4	Journey 5	6-8	Daily statement
Journey average: v / km/h	15.44	15.40	16.68	14.57	17.38	...	16.33
Max. speed.: v / km/h	63.47	58.70	65.88	65.58	65.70	...	61.16
Acceleration. max.: a / ms ⁻²	1.17	1.36	1.55	1.41	1.19	...	1.35
Delays. max.: a / ms ⁻²	1.54	1.66	1.65	1.38	1.29	...	1.42
Total measuring time: t / min	41.0	45.0	38.0	47.7	36.3	...	5h 26min
Journey duration (v>0): t / min	25.9	25.2	25.0	25.1	24.3	...	3h 25min
Route length / km	10.8	11.8	10.8	11.8	10.9	...	88.7

Table 4-1: Key data for the Journey Profile and Speed

Table 4-1 gives an overview of the key data for the first individual cycles on the 08.10.2014. The daily statement contains the total operational duration of journeys 1 to 8. The average value for the journeys in km/h relates to the average cycle speed whereby stops and traffic-related standstill times are included. This leads to the previously mentioned average cycle speed at SORT-2-Level. In addition, the pure journey time is presented, which doesn't include the standstill times within this information. With the route distances the slight difference between the cycles for outward and return journeys is apparent. Since these distances are not identical, this results in all subsequently calculated values corresponding to the route section of the total measurement.

4.1.1 Performance in Intermediate Circuit

The course of the performance output (drive, additional consumers) measured by the Supercaps during the journey / the performance recording (braking/recuperation, charging) is presented in Fig. 4-7 (blue) for the start of the journey and the speed (red) is presented with the same scaling as a base reference.

In order to test the plausibility a longitudinal dynamics model was used to calculate or estimate the required traction performance at the wheel on the basis of the velocity course measured (black). Since this model considers neither the height profile nor the active additional load and the additional consumers and serves merely for valida-

tion purposes, deviations can naturally be expected; in addition there is a differentiation between the wheel and capacitor performance through losses in power, the electric motors, the on-board power supply network as well as the additional consumer demand.

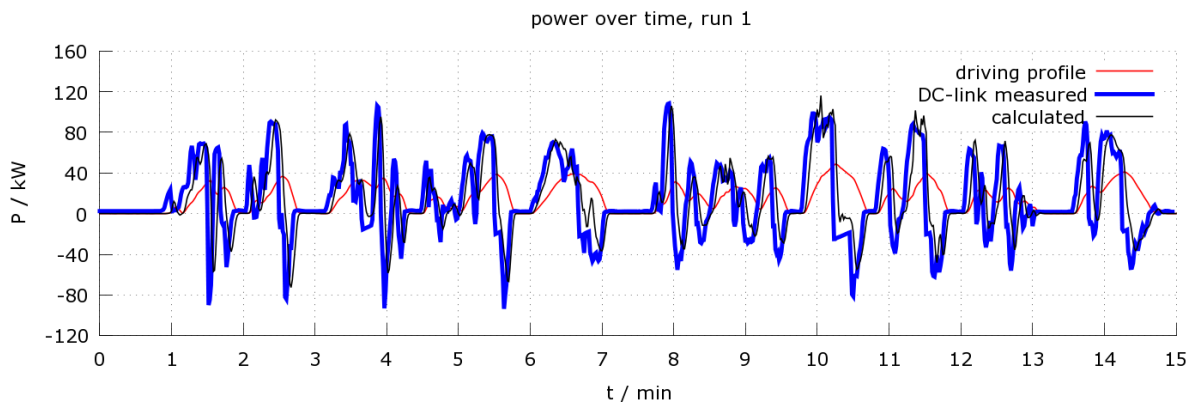


Figure 4-7: Performance at the Supercap, Start of Journey 1

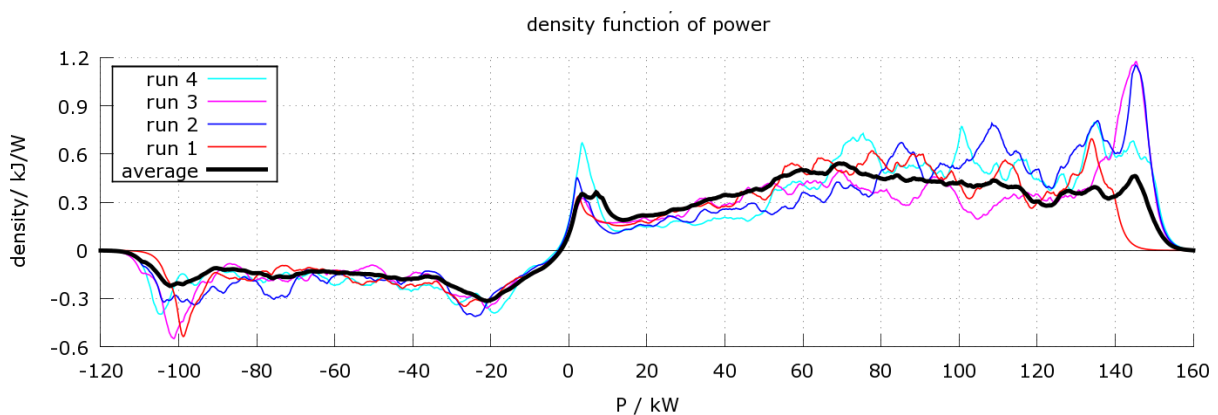


Figure 4-8: Energy-related distribution of the drive power at the Supercap

In order to be able to analyse the energy turnover better, a density function for the performance curve was calculated for each journey (see Fig. 4-8). In contrast to the analysis of the speed, however, there is no time weighting factor; instead the converted energy is used. The area below the density function also specifies in intervals e.g. of 0 to 160kW how much energy has been converted in this area. With the axle scaling used 1 casket equates as follows:

$$E = 20 \text{ kW} \cdot 0,3 \frac{\text{kJ}}{\text{W}} = 6 \text{ MJ} = 1,67 \text{ kWh}$$

The surface for the total positive power range thus corresponds to the total energy required for the power unit plus additional consumers. In this case, the black curve denotes the average of all journeys. For the total negative power range the energy recovered during operational status in the capacitor is received, i.e. the braking energy at the wheel *minus* losses and additional consumer demand. Through the extreme change between acceleration and braking without quotas for journeys at constant speed, a higher recovery rate of up to 30% should result as expected. As previously mentioned a lower average speed has a negative effect on both consumption and the supercap recovery level.

NB: energy is converted into heat through the almost static tractional resistance (air resistance, rolling friction) and the conversion losses in driving, which cannot, in principle, be recovered. Using the performance curves in Figure 4-7 (calculation of battery power versus wheel power) it can be seen that electric braking is probably the predominant form used. This is very advantageous for a low energy consumption, nevertheless the condition of the mechanical brakes should be monitored (corrosion).

Peaks in the density function indicate that much energy is being converted in the corresponding power range. The spectrum of the capacitor performance ranges from approx. -110 kW (brakes) to approx. 150 kW (drive power).

Finally, the performance demand of additional consumers should be investigated. This can be calculated directly on the measuring device itself. For the analysis at the measurement point on the supercap the time segments for the performance over time during drive operation (criteria $v > 0$ and $a \neq 0$) were removed. A graphic analysis is done with the aid of a density function (see Fig. 4-9). As can be seen from the peaks in the density function, the additional consumers should be found in the areas 2 kW, 3 kW, 7 kW and 8.5 kW.

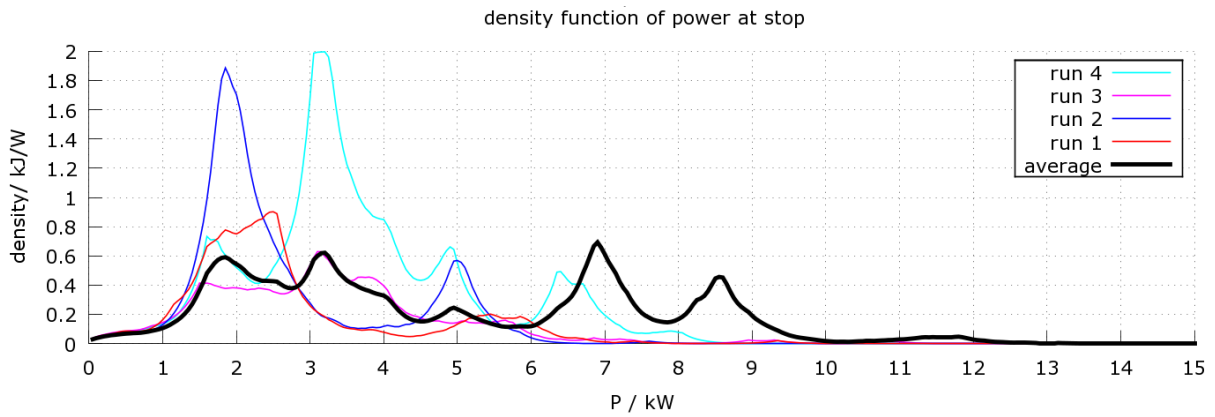


Figure 4-9: Density distribution of the additional consumer demand

Due to the multitude of additional consumers measured a differentiation is taken into consideration in the following.

4.3.1.1 Air conditioning

Figure 4-10 shows the performance recording of the air conditioning taken at Measurement Point M4 on the 08.10.2014. On average, the performance here reaches 0.3kW. Due to the advantageous ambient temperatures (see Chapter 3) the air conditioning was not on during real operation (automatic function) and thus shows the following progression.

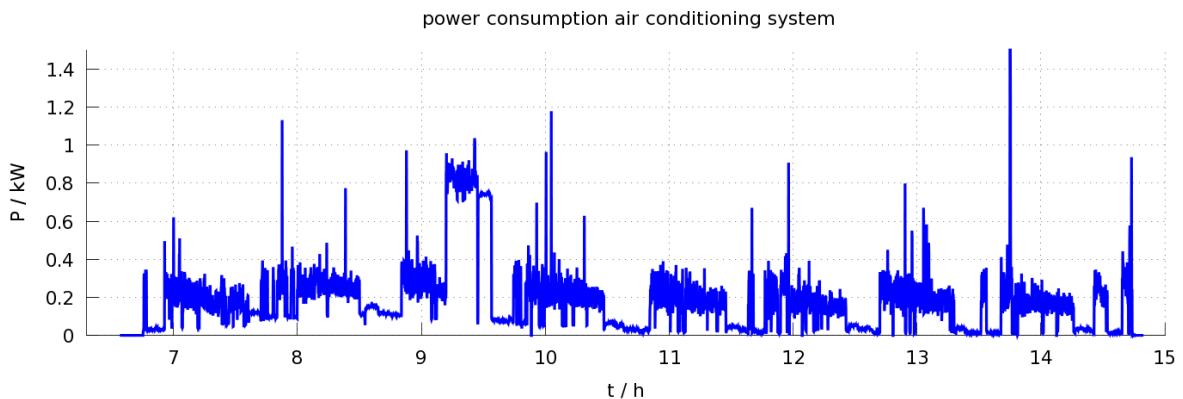


Figure 4-10: Performance recording for the air conditioning unit in real operation (automatic)

In order to calculate the potential performance on the basis of the given conditions the heating was switched on during one journey and the air conditioning was switched to manual operation. Figure 4-11 clearly shows that with the air conditioning switched on the performance recorded increases noticeably and is in the range of 5 to 6 kW.

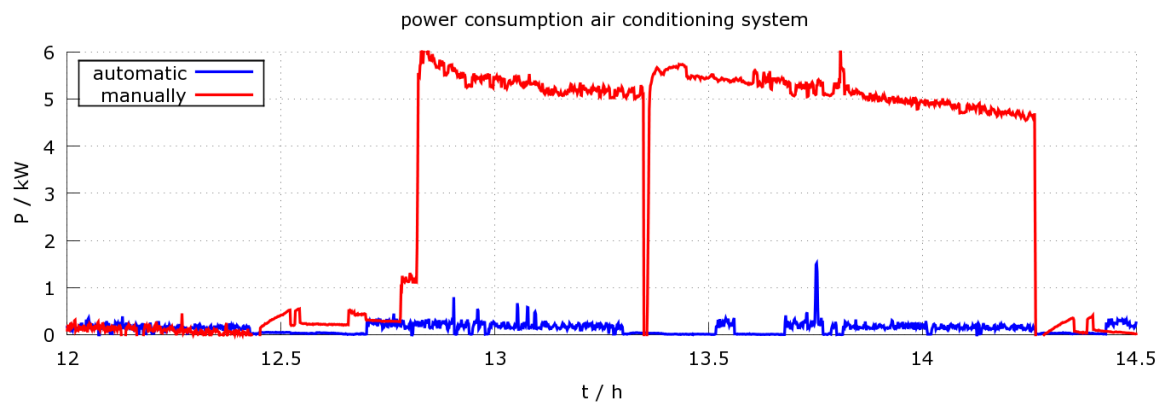


Figure 4-10: Performance record of the air conditioning in real operation (automatic)

4.3.1.2 Air compressor and oil pump

A constant ratio resulted from the measurements of the performance recording of the permanent additional consumers, air compressor and oil pump, which were taken at Measurement Point M5. Figure In 4-11 clearly shows that one consumer ranges between 1 and 1.5kW, cutting off only during charging and the second consumer alternates between 1 and 4.5kW. It can be assumed that this involves a highly variable consumer around the air compressor which is only active when reacting to a fall in pressure whereas the oil pump, in contrast, is permanently active throughout the journey. Both of these consumers can clearly be seen in the density distribution in Figure 4-9. Since only one Measurement Point was available in this case, a colour differentiation is not possible.

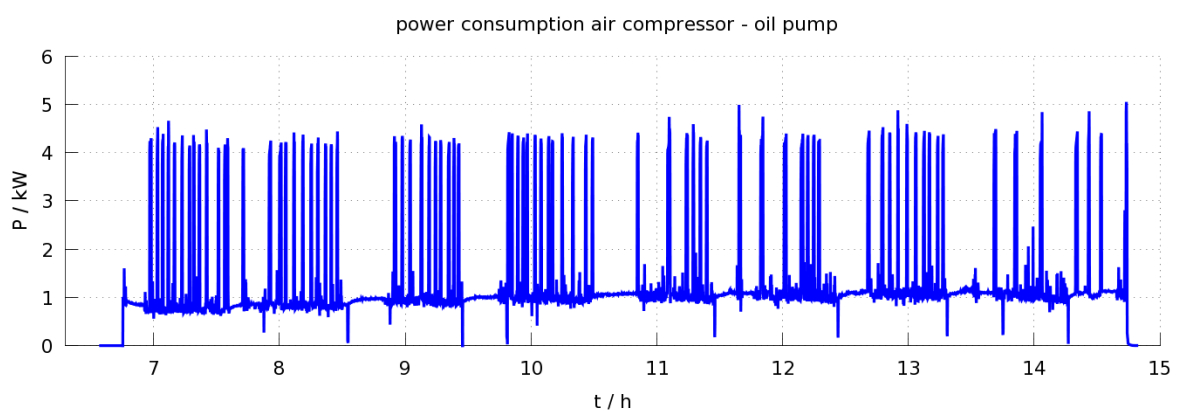


Figure 4-11: Performance record for the air compressor and the oil pump

4.3.1.3 24V-Power Supply System

The 24V-Power Supply System was measured using a DC/DC converter and shows an unremarkable as well as distinct ratio. The down peaks for switch-off/switch during the charging process are recognisable and these correspond exactly with the down peaks shown previously in Figure 4-11. The performance record ranges in this case between 0.5 and 1.5kW.

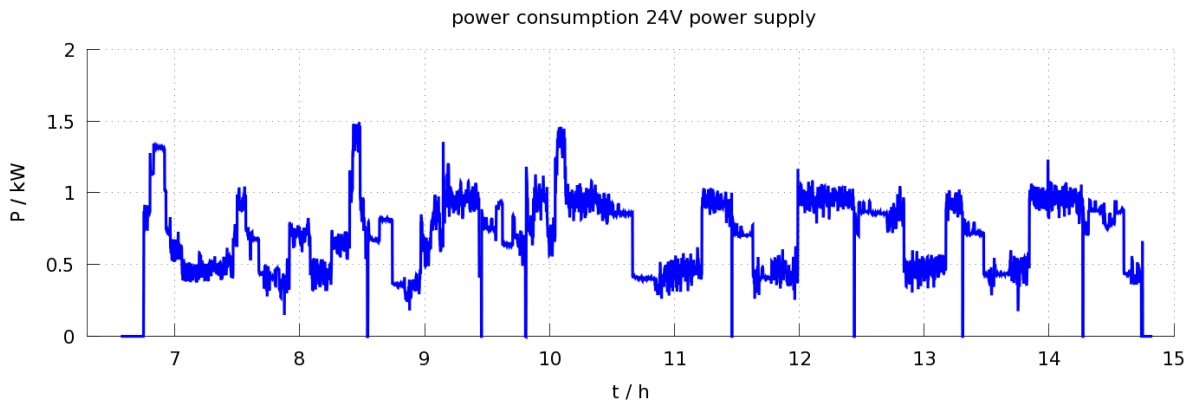


Figure 4-12: Performance record for the 24V Power Supply System

4.3.1.4 Cooling Super-Caps

The cooling of the capacitors was not measured separately due to the “loss character” in relation to the system effectiveness of the capacitors. When considering the density distribution for the additional consumers during standstill, it can be assumed that the cooling ranges between 2.5 and 4.5 kW, since this range was not represented during the first two cycles, but does, however, develop progressively during the subsequent cycles.

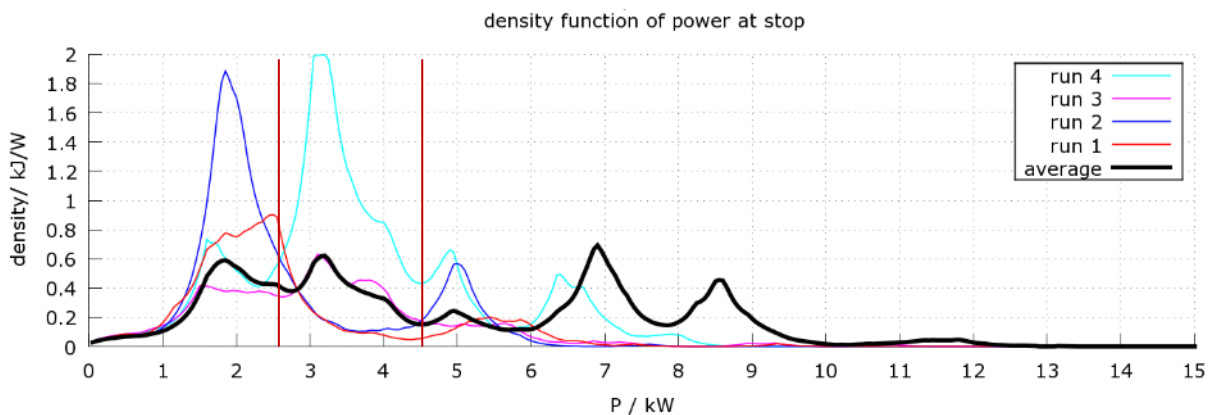


Figure 4-13: Density distribution of the additional consumer performance (Section: cooling)

4.3.2 Energy Consumption

The energy turnover is derived from the performance measured in the intermediate circuit (integral to the performance via the time interval of the measurement i.e. surface below the curve). In contrast to Chapter 4.3.2., the energy fed into the battery during charging or recuperation is counted as positive and that energy power taken from the capacitor for drive power is counted as negative. In this case the following should be taken into consideration for the time intervals of the individual processes:

Charging: $\Delta E = E_{\text{charging}} = \text{positive (charging capacitor)}$

Driving: $\Delta E = E_{\text{braking}} \text{ (charging, positive)} + E_{\text{drivepower}} \text{ (discharging, negative)}$
= total negative

The recuperation level is the quotient from $\Delta E_{\text{braking}}$ to $\Delta E_{\text{drivepower}}$.

In the following the daily statement from the measuring points at the supercap (M2) and at the pantograph (M1) are presented.

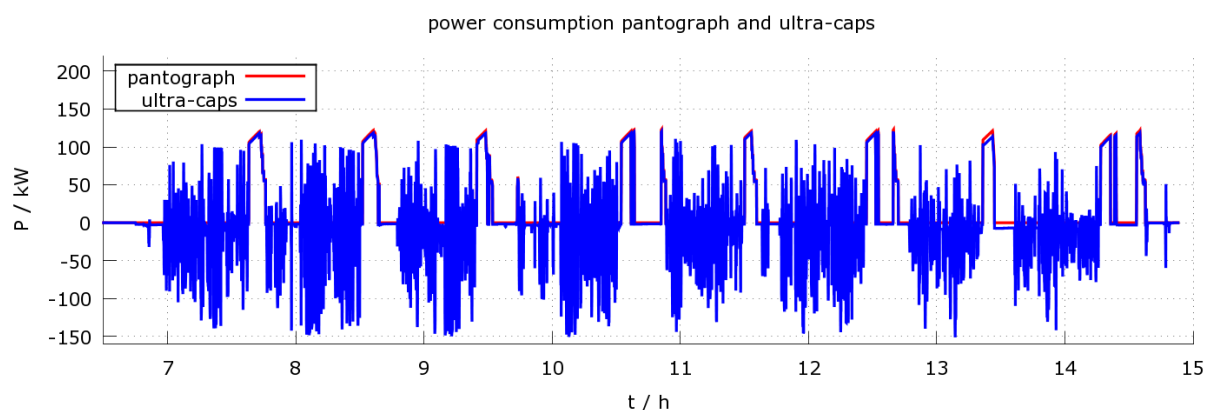


Figure 4-11: Performance intake/-output in the daily cycle at the pantograph and supercapacitor

Here, it can clearly be seen when the charging cycles occur (red); these dip almost exactly with the incoming performance peaks at the supercapacitor. If this deviation were clearly visible here, this would signify heavy losses during charging.

As already mentioned at the start, the degree of efficiency of the charging stations is not taken into consideration at this juncture. The measurement between M1 and M2 merely includes the HV on board power supply whereby a higher degree of efficiency

could be assumed. This was confirmed by the measurement. Likewise, the energy recorded is presented in Figure 4-12.

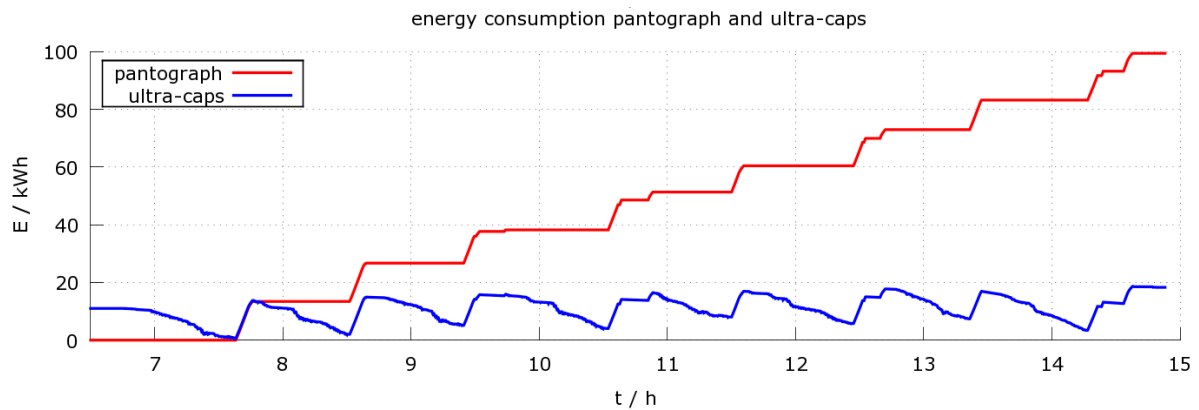


Figure 4-12: Energy balance daily cycle at the pantograph and supercapacitor

At the start of the measurement the supercaps were already charged and start-up was immediate whereby the energy recording from the pantographs was also set at zero. In the first charging cycle it can clearly be seen that the charging at both the capacitor and the pantograph tally with one another. The progression of the capacitor also shows that it is slowly increasing. Thus, the energy range of the capacitor is displaced. Possible causes for this ratio could be a reaction by the dielectric fluid to the increasing temperatures in vehicle operation, or also to a change in the ohmic resistance of the electrodes during warming. However, this has no effect on the effectiveness of the supercaps since the absolute charging remains constant and, thus, the behaviour of the total system is not affected.

Date	08.10.14						
Status	Journey 1	Journey 2	Journey 3	Journey 4	Journey 5	6-8	Daily statement
Measuring Point	Measuring Point2: Ultra-Caps						
P _{max} discharging / kW	<i>-140.6</i>	<i>-150.5</i>	<i>-149.7</i>	<i>-150.6</i>	<i>-147.7</i>	...	-147.6
P _{max} charging / kW	<i>103.6</i>	<i>109.5</i>	<i>110.0</i>	<i>108.0</i>	<i>111.8</i>	...	107.0
E _{Supercap Output} / kWh	<i>-15.51</i>	<i>-18.17</i>	<i>-15.58</i>	<i>-18.05</i>	<i>-13.54</i>	...	-125.34
E _{Supercap Recording} / kWh	<i>5.75</i>	<i>6.40</i>	<i>5.98</i>	<i>6.17</i>	<i>5.09</i>	...	40.8
Δ Energie _{Supercap} / kWh	<i>-9.76</i>	<i>-11.77</i>	<i>-9.60</i>	<i>-11.88</i>	<i>-8.45</i>	...	-84.6
E _{Pantograph charging} / kWh	<i>13.42</i>	<i>13.30</i>	<i>11.53</i>	<i>13.12</i>	<i>9.13</i>	...	99.5
Time / min	<i>41.0</i>	<i>45.0</i>	<i>38.0</i>	<i>47.7</i>	<i>36.3</i>	...	5h 26min
Route length / km	<i>10.8</i>	<i>11.8</i>	<i>10.8</i>	<i>11.8</i>	<i>10.9</i>	...	88.7
Recuperation / %	<i>37.1</i>	<i>35.2</i>	<i>38.4</i>	<i>34.2</i>	<i>37.6</i>	...	32.2
Consumption / kWh/km	<i>0.91</i>	<i>1.00</i>	<i>0.89</i>	<i>1.01</i>	<i>0.78</i>	...	0.95
Consumption / kWh/min	<i>0.24</i>	<i>0.26</i>	<i>0.25</i>	<i>0.25</i>	<i>0.23</i>	...	0.26

Table 4-2: Key data daily statement at Measuring Point M2: Supercap

The total daily energy balance is shown in Table 4-2 in figures. The daily statement in Table 4-2 contains 8 cycles. The total duration measured for the 8 cycles is 5 hours 26 minutes which corresponds to an average 41 minutes per journey. The figures in italics correspond to individual data from the first 5 journeys.

The supercap was systemically charged during each of the charging processes, as far as possible (see Chapter 2).

Thus the degree of effectiveness of the supercap can be calculated as follows:

$$\eta_{Supercap} = \frac{E_{OUT}}{E_{IN}}$$

$$\eta_{Supercap} = \frac{E_{Supercap\ output}}{E_{Pantograph\ charging} + E_{Supercap\ recording}}$$

$$\eta_{Supercap} = \frac{125.34}{99.5 + 40.8}$$

$$\eta_{Supercap} = 89.3 \%$$

From the measurements recorded from the individual consumers the energy for the whole daily cycle can be calculated:

- Through the charging between cycles the **Pantograph** supplies, in total, **99.5 kWh** as shown in Figure 4-12.
- The **Electric motors** consume **67.5 kWh** (see Figure 4-13).
- The **Air conditioning unit (AC)** consumes **1.5 kWh** (see Figure 4-14).
- Both of the additional consumers **Air compressor** and **Oil pumps** consume a combined total of **12.3 kWh** within the total daily cycle (see Figure 4-15).
- The last measured consumer is the on board 24V power supply network (**Low-Volt-Network**) with a total energy consumption of **5.7 kWh** (see Figure 4-16).

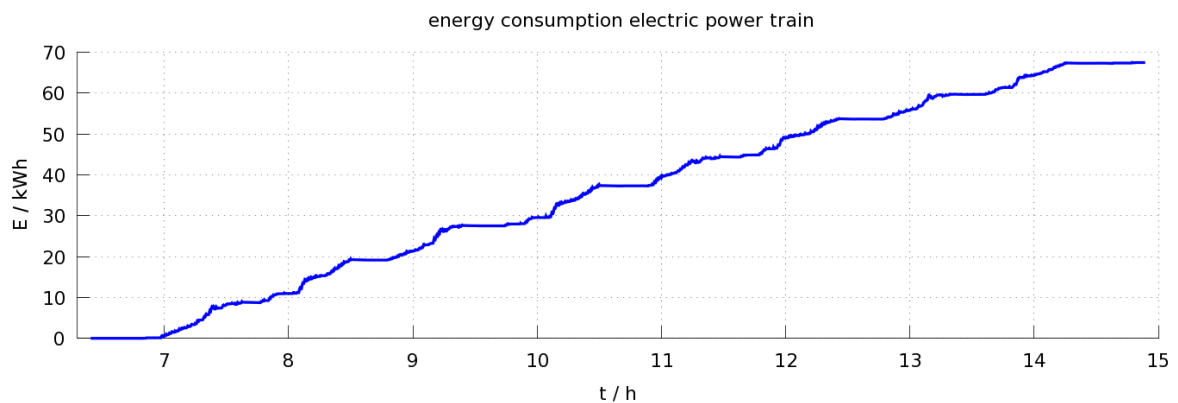


Figure 4-13: Energy balance daily cycle at Measuring Point M3: Electric motor

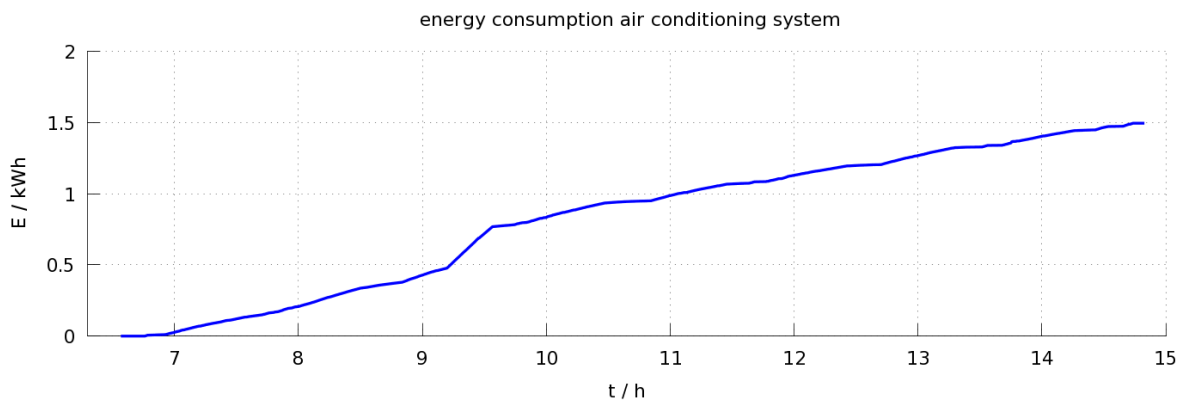


Figure 4-14: Energy balance daily cycle at Measuring Point M4: air conditioning

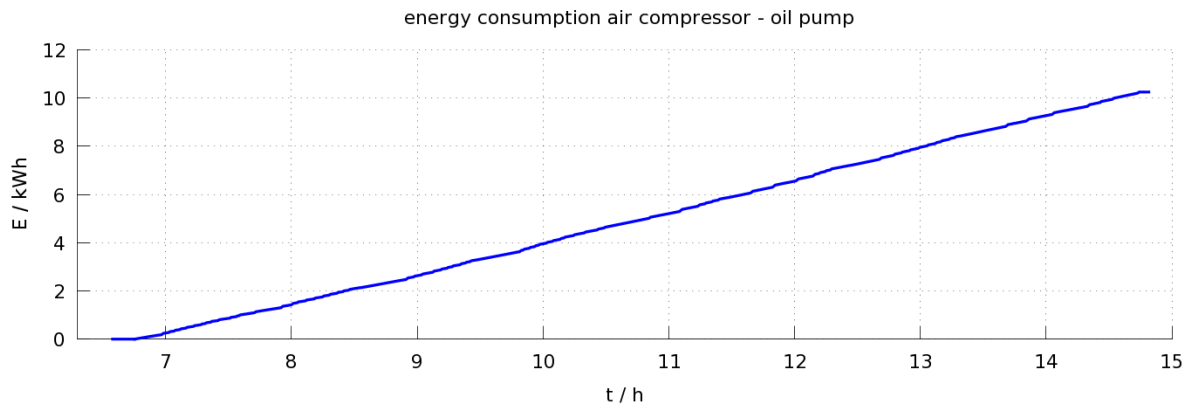


Figure 4-15: Energy balance daily cycle at Measuring Point M5: air compressor and oil pump

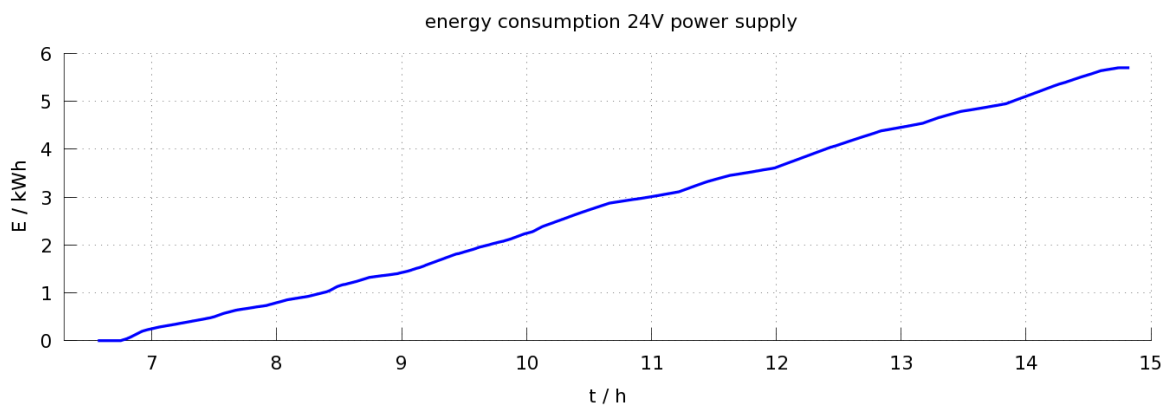


Figure 4-16: Energy balance daily cycle at Measuring Point M6: 24 V On board power supply

Thus, the efficiency factor of the system can be calculated from the **pantograph** to the electric motor (**Electric Power Train**) as follows:

$$\eta_{Pan-EPT} = \frac{E_{OUT}}{E_{IN}}$$

$$\eta_{Pan-EPT} = \frac{E_{EPT} + E_{AC} + E_{Air,Oil} + E_{24V}}{E_{Pantograph\ charging}}$$

$$\eta_{Pan-EPT} = \frac{67.5 + 1.5 + 12.3 + 5.7}{99.5}$$

$$\eta_{Pan-EPT} = 85.4 \%$$

In the process the cooling of the supercaps is balanced in the form of a loss. A detailed consideration of the E-Bus system is not possible due to the lack of measure-

ments at the charging station as well as information on the gears and the degree of efficiency of the E-Motors.

4.4 Summary

The energy consumption measurement produced the following conclusive key data:

Vehicle

Power range:	-110 kW ... +150 kW, brake/power units
Brake energy recuperation:	32.2 % (based on the Supercaps)
Total energy consumption:	0.95 kWh/km or 0.26 kWh/min

Supercap Charging:

Charging period:	approx. 1h
Charging capacity at the pantographs:	max. 120 kW

5 Simulated Calculation of the Energy Demand on Line 11

In order to compare the energy consumption measured (see Chapter 4), the energy consumption was simulated independently of additional load and air conditioning using the GPS data recorded on Line 11.

5.1 Description of the Simulation Model Applied

In order to determine the energy demand a model of the longitudinal dynamics shown in Figure 5-1 was applied. The propulsion F_Z must overcome the tractional resistance F_W i.e. the total of all resistances affecting the vehicle:

$$F_W = F_{WR} + F_{WL} + F_{WSt} + F_{WB}$$

with:

F_W : Tractive resistance (Total of all resistances)

F_{WR} : Wheel resistance

F_{WL} : Drag

F_{WSt} : Gradient resistance

F_{WB} : Acceleration resistance

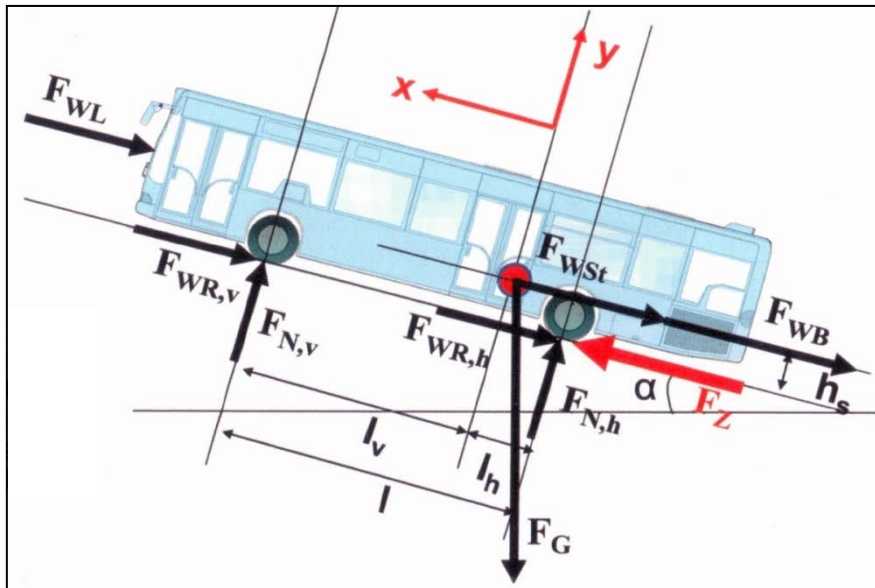


Figure 5-1: Tractive resistance and tractive force on the urban bus (Source: Pütz)

The tractive resistance significantly influences the driving performance and the fuel consumption of an urban bus. Variables such as achievable acceleration, maximum speed, climbing power etc. can be determined using equilibrium ratios between tractive force and tractive resistance.

The power P_{Demand} required to overcome the tractive resistance is comprised of the percentages of the rolling, air, climbing and acceleration resistance, the losses for wheel slippage and in the power transmission as well as the power demand for operating the auxiliary equipment and it results from multiplying the abovementioned tractive resistances with the vehicle speed v :

$$P_{Demand} = P_R + P_L + P_{St} + P_B + P_{slippage} + P_{transmission} + P_{auxilliaris}$$

The power P_R required to overcome the rolling resistance which is the dominating wheel resistance is dependent on the mass m of the vehicle ($m_{vehicle}$) and the load capacity ($m_{loading}$) as well as on the rolling resistance coefficients ($f_{r0}; f_{r1}; f_{r4}$), the degree of incline α and the travelling speed v (g = acceleration due to gravity):

$$P_R = (m_{vehicle} + m_{loading}) \cdot g \cdot (f_{r,0} + f_{r,1} \cdot v + f_{r,2} \cdot v^4) \cdot \cos\alpha \cdot v$$

The air resistance output is characterised by factors inherent in the vehicle profile: c_W value, average surface area of the vehicle A , air density ρ_L (1,2 kg/m³), travelling speed v_F as well as the wind speed v_S :

$$P_L = 0,5 \cdot c_W \cdot A \cdot \rho_L \cdot (v_F + v_S)^3$$

The power required to overcome the climbing resistance is dependent on the mass of the vehicle $m_{vehicle}$ and the load capacity $m_{loading}$ as well as the degree of incline α and the travelling speed v :

$$P_{St} = (m_{vehicle} + m_{loading}) \cdot g \cdot \sin\alpha \cdot v$$

In order to accelerate the vehicle translatively using the acceleration a , the vehicle mass $m_{vehicle}$ and the load capacity $m_{loading}$ are accelerated gyrationally. For the calculation of the gyration into translative acceleration the equivalent mass m_{Red} is introduced:

$$P_B = (m_{vehicle} + m_{loading} + m_{Red}) \cdot a \cdot v$$

However, electric vehicles use the energy from the storage unit not only for the drive transmission but also for other consumers such as the auxiliary components (e.g. power steering pump, brake power, shock absorbers), door control and air conditioning/heating. If the total of all required power is negative at any time then the corresponding sum of energy can be recovered in part (see Figure 5-2).

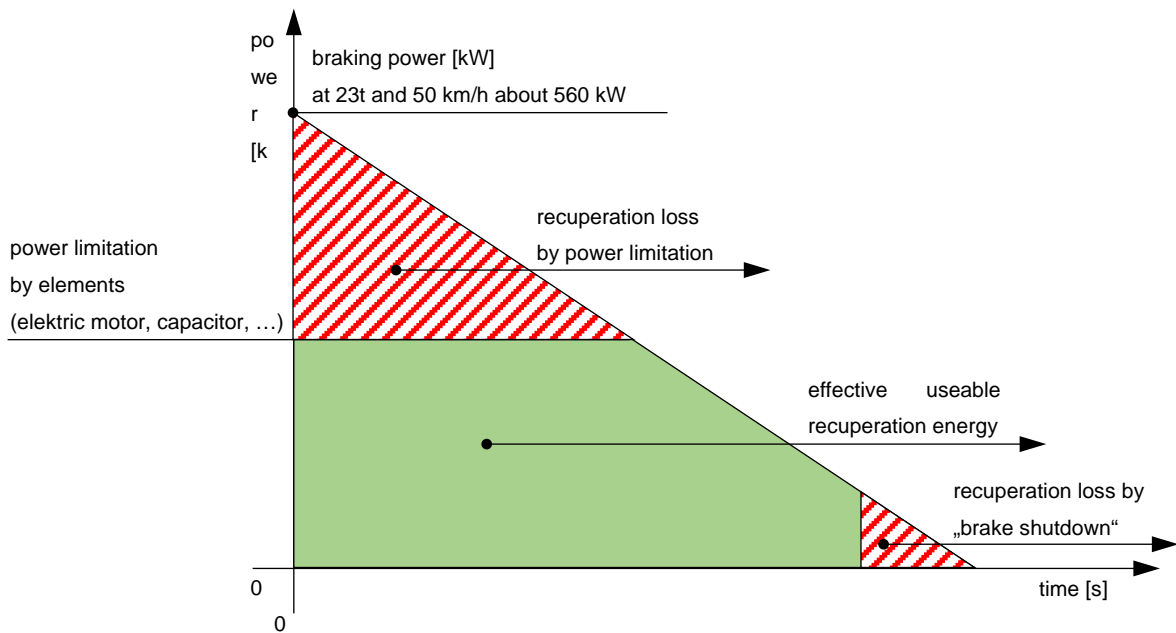


Figure 5-2: Recovery losses through heavy braking (source: ISEA, translated)

In this case, the supercap should demonstrate a clear advantage over E-busses with batteries since the wire density is significantly greater and therefore significantly increases the performance limit through the components.

5.2 Simulation of the Energy Demand on Line 11

The data required for the simulation was recorded on the 07.10.2014 and 08.10.2014. In order to achieve a better comparison of the energy consumption measured, only the journeys from the second measurement day are presented. The following data on the power consumption was calculated for all 8 cycles during this day.

5.2.1 Scenario 1: 100% Occupancy Rate

In the first observation an **occupancy rate of 100%** with the **air conditioning** in operation was assumed (100% power consumption). In order to calculate the total mass of the vehicle load the unladen weight of the bus (approx. 12.5t) and the total weight

of the laden vehicle (inc. driver) were applied (in total 18t). In addition, for safety purposes, a “worst case scenario“ consideration of the pure energy demand with air conditioning and without brake energy recuperation was carried out. The following Figure 5-3 shows the energy demand using the example of cycle 1. The individual energy demand components are presented in summary.

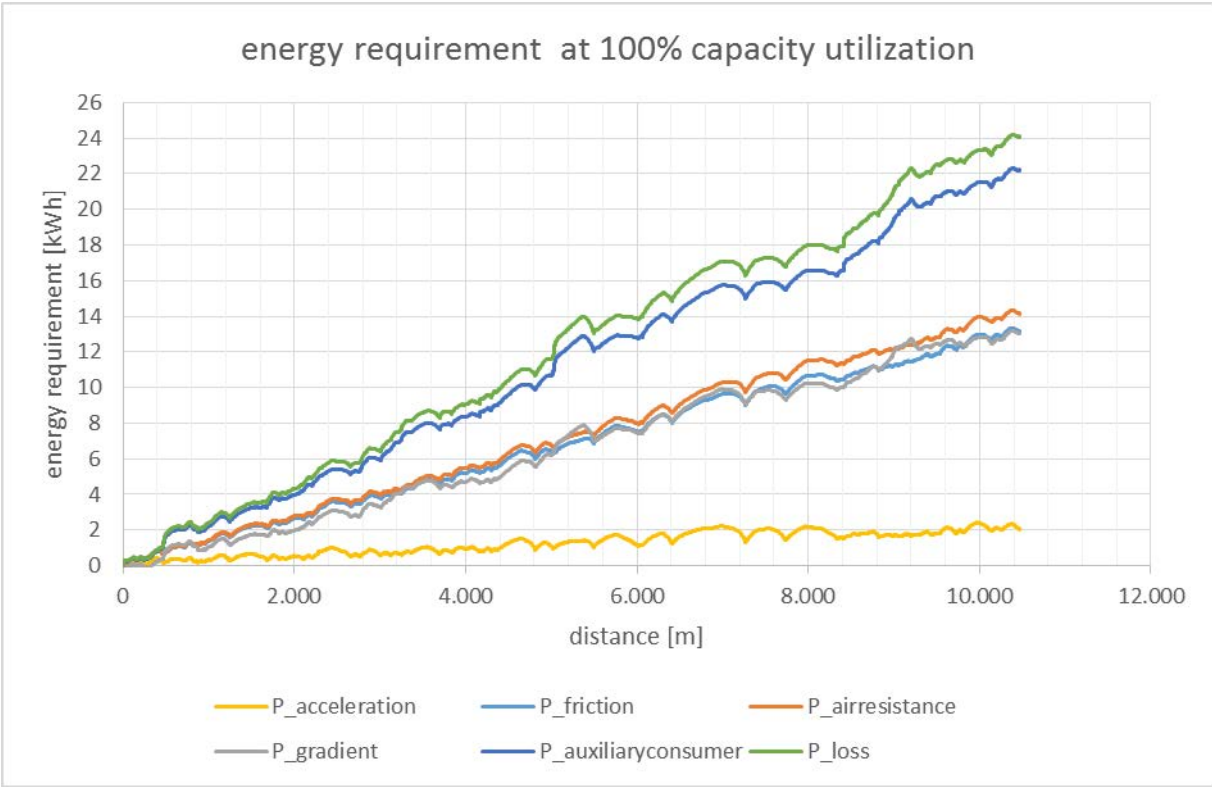


Figure 5-3: Differentiated energy consumption at 100% occupancy rate with air conditioning on and without brake energy recuperation (cycle 1)

Thus, a calculated energy demand of **2.28 kWh/km** without recuperation, results for Line 11 measured in Sofia, corresponding to 25.3kWh for one full circuit. With a total capacity of 20kWh no complete cycle would, consequently, be possible without recuperation.

With an applied **brake energy recuperation of 30%** (cf: measurements 32.2%) the specific energy consumption would drop to around **1.60 kWh/km** whereby 1 circuit with full occupancy would be feasible with a remaining charge of 11.3%.

5.2.2 Scenario 2: 25% Occupancy Rate

For a typical urban transport company an **occupancy rate of 25%** can be assumed on average for routine operation. On both days in Sofia this typical occupancy rate was found to be slightly different, corresponding to an additional load of 1500 kg (20 passengers). A worst case scenario with air conditioning and without brake energy recuperation is thus assumed in this instance.

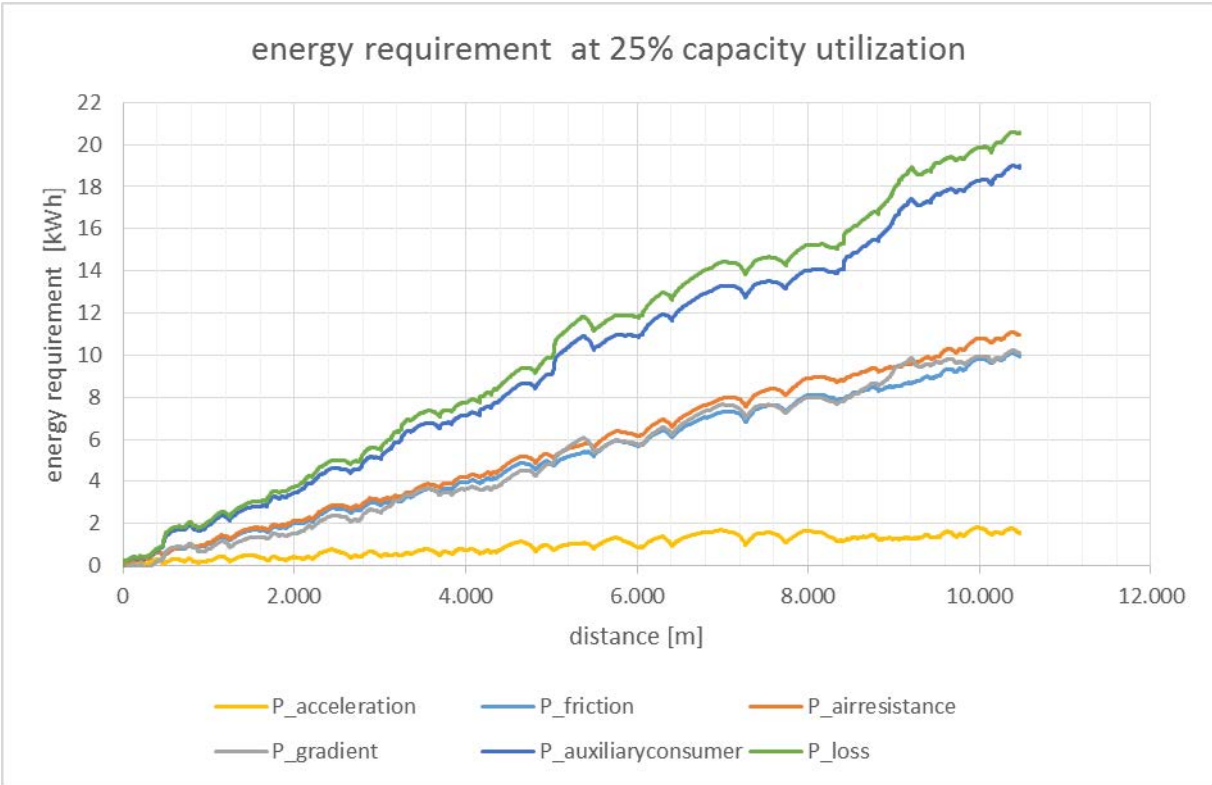


Figure 5-4: Line 11: Energy consumption (total) at 25% occupancy rate in operation with air conditioning on and without brake energy recuperation (cycle 1).

Thus, for an occupancy rate of 25% an energy demand of **2.04 kWh/km** results, i.e. for a circuit of 22.7kWh in total.

With an assumed recuperation rate of 30% an occupancy rate of 25% with full air conditioning operation 1 cycle would be feasible.

5.3 Summary Tables showing the most important simulation energy demand results

Occupancy rate	Air conditioning	Specific Consumption	Energy	Absolute Energy Consumption	Cycles	Residual Charge
	Yes/No	kWh/km		kWh/cycle	-	%
100%	Yes	2.28		25.35	0	100
100%	No	1.67		18.55	1	7.24
25%	Yes	2.04		22.67	0	100
25%	No	1.43		15.88	1	20.6

Table 5-1: Summary of the Simulation Results without Recuperation

As a result, the energy consumption measurement shows that the Chariot eBus achieves a recovery rate of around 30% which was applied during the simulation:

Occupancy rate	Air conditioning	Specific Consumption	Energy	Absolute Energy Consumption	Cycles	Residual Charge
	Yes/No	kWh/km		kWh/cycle	-	%
100%	Yes	1.60		17.74	1	11.3
100%	No	1.17		13.00	1	35.1
25%	Yes	1.43		15.87	1	20.7
25%	No	1.00		11.11	1	44.4

Table 5-2: Summary of the Simulation Results with Recuperation

Subject to the results of the simulation the Chariot eBus could be introduced with a recuperation of 30% (see Table 5-2) even with a full occupancy rate and the air conditioning on in real operation without any misgivings.